5-2011

The Effect of Ultraviolet Light on Cell Viability, DNA Damage and Repair in Hutchinson-Gilford Progeria Syndrome and BJ Fibroblasts.

McKayla Johnson
East Tennessee State University

Follow this and additional works at: https://dc.etsu.edu/honors

Part of the Molecular Biology Commons

The Effect of Ultraviolet Light on Cell Viability, DNA Damage and Repair in Hutchinson-Gilford Progeria Syndrome and BJ Fibroblasts

A thesis presented to
The faculty of the Department of Biological Sciences
East Tennessee State University

In partial fulfillment of the requirements for the
Honors-in-Discipline Biology Program and the
Talent Expansion in Quantitative Biology Program

By McKayla Brianne Johnson
May 2011

Dr. Phillip R. Musich, Chair
Dr. Anant Godbole
Dr. Yue Zou

Key Words: UV DNA Damage, UV DNA Repair, Pol-η, HGPS, DDB-2

Abstract

The Effect of Ultraviolet Light on DNA Damage and Repair in Hutchinson-Gilford Progeria Syndrome and BJ Fibroblasts

By: McKayla Johnson

Patients of Hutchinson-Gilford Progeria Syndrome (HGPS) display a rate of aging up to ten times that of normal human populations. It might be expected that HGPS cells would have a decreased ability to repair DNA damage through the cell cycle as compared to normal cells such as those of the BJ cell line since DNA damage accumulation is a hallmark phenotype of aging. On earth, we are exposed to far more ultraviolet-B (UV-B, 280-315 nm) and UV-A (315-400 nm) than UV-C (100-280 nm) radiation, since the latter is filtered-out by the atmospheric ozone layer. The relative sensitivity of prematurely aging HGPS cells to UV-B irradiation is unknown. It was hypothesized that the normal fibroblast cell line (BJ) would exhibit a higher rate of DNA repair and a higher level of cell viability after exposure to ultraviolet radiation than would be observed with the HGPS cells, and that these differences would be greater as the HGPS cells age in culture. A Cell-Titer Blue Viability Assay (Promega) was used to determine the effect of UV-B and UV-C on metabolic activity, an indicator for cell viability, in HGPS, BJ, and A549 (a human lung carcinoma) cells. A translesion DNA synthesis protein, pol-η, and several other DNA transcription and repair-related proteins also were hypothesized to be altered in the HGPS cell line, both before and after UV-induced DNA damage, as compared to the BJ cell line. Western blotting was used to monitor these proteins in BJ and HGPS cells following UV-C exposure. No differences in short-term viability were observed between BJ and HGPS cells, reflecting similarities in their repair abilities on the cellular level; however, there were significant differences in long-term viability.   Enzyme Linked Immunosorbant Assays (ELISA) revealed a significant difference in DNA repair at the molecular level. Moreover, Western blotting revealed differences in the amounts of several repair-related proteins following UV exposure, including pol-η, an important trans-lesion synthesis protein. Although the difference in DNA repair did

not appear at the cellular level, it is apparent that HGPS cells show a greater sensitivity to both UV-B and UV-C irradiation as compared to normal BJ fibroblasts and A549 carcinoma cells.

Table of Contents

List of Tables

List of Figures

List of Abbreviations

Ultraviolet Light, A, B, C	UV, UV-A, -B, -C
Cyclobutane Pyrimidine Dimer	CPD
[6-4] Photoproduct	[6-4] PP
Nucleotide Excision Repair	NER
Global Genomic Nucleotide Excision Repair	GG-NER
DNA Polymerase η (Pol-eta)	Pol-η
DNA-Damage Binding Protein, 1, 2	DDB, -1, -2
DNA damage response	DDR
Hutchinson-Gilford Progeria Syndrome	HGPS
Xeroderma Pigmentosum	XP
Eagle's Minimal Essential Media	EMEM
Fetal Bovine Serum	FBS
Phosphate Buffered Saline	PBS
Bovine Serum Albumin	BSA
Dulbecco's Minimal Essential Media	DMEM
Urea Sample Loading Buffer	USLB
Tris-Buffered Saline with Tween-20	TBST
Trichloroacetic Acid	TCA
Ethylene-diamine Tetraacetic Acid	EDTA
Tris-EDTA	TE
Enzyme Linked Immunosorbent Assay	ELISA

Chapter 1. INTRODUCTION

Skin cancer has become a growing concern for Americans with more than two million people being diagnosed every year, and has become the most common type of cancer in Americans. Studies by The Skin Cancer Foundation report that one in every five individuals in the United States will develop skin cancer in the course of their lifetime (www.skincancer.org). A particular cause can be directly correlated to ultraviolet light (UV) exposure, with the most prominent source being the sun. 90% of all non-melanoma skin cancers are attributed to UV exposure. Traits commonly associated with aging, such as wrinkles and uneven pigmentation, also are attributed to UV exposure[1]. In addition, the vast majority of mutations found in melanoma skin cancer patients are caused by UV irradiation.

Ultraviolet light causes two major bulky base-adducts: cyclobutane pyrimidine dimers (CPDs) and [6-4] photoproducts ([6-4] PPs) (Figs. 1, 2). During replication, human DNA polymerase III stops at these bulky base-adducts because it is unable to replicate past them. In order to continue with DNA replication, a nucleotide excision repair (NER) DNA repair process must first occur.

Fig.1. UV creates a bulky base adduct in DNA.
http://www.sciencebuddies.org/science-fair-projects/project_ideas/MicroBio_p017.shtml

DNA Polymerase η (Pol-η (Pol-eta)), a member of the Y family of DNA polymerases, is a trans-lesion polymerase protein which mediates the bypass of bulky lesions induced by UV irradiation and some chemotherapeutic agents (Table 1)[3]. Studies have shown that the level of Pol-η is regulated by ubiquitination and proteasome-
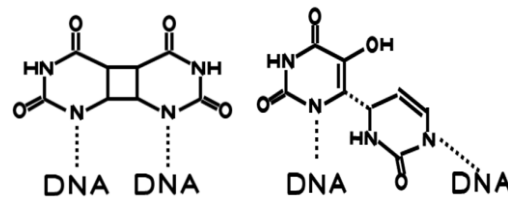
Fig. 2. Diagram of bulky base adducts. CPD (left). [6-4] PP (right).

mediatiated degradation after translation[2]. Pol-η is encoded by the Pol H gene in humans, and is distributed uniformly in the nucleoplasm. After UV exposure, it forms intranuclear foci and colocalizes with the replication protein PCNA at CPD sites[3]. Pol-η is responsible for synthesis
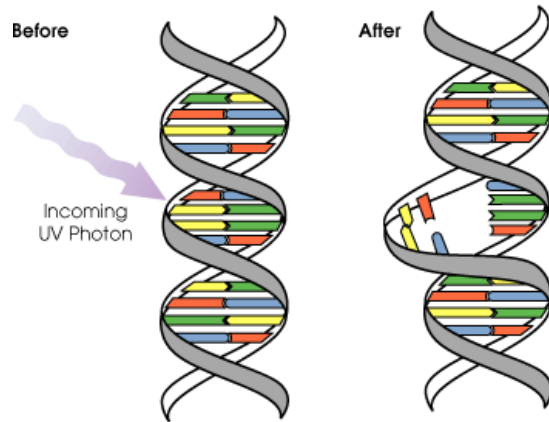
over these bulky-base adducts that DNA polymerase III cannot bypass. Pol-η repairs CPDs most efficiently, and was previously referred to as error free; however, it is somewhat inefficient when repairing [6-4] PPs[3]. Therefore, a lack of Pol-η could result in high levels of mutations due to replication errors stemming from UV damage.

Following UV irradiation, the trans-lesion pathway occurs. These UV-induced lesions are [6-4] PPs and CPDs. During DNA

Name	Family[a]	Proposed main function	Misincorporation per nucleotides[b]
γ	A	Mitochondrial DNA replication	10^{-6}
θ	A	DNA repair	–
α	B	DNA replication priming	10^{-4}
δ	B	DNA replication	10^{-5}
ε	B	DNA replication	10^{-6}
ζ	B	Bypass synthesis	10^{-4}
β	X	Base excision repair	5×10^{-4}
λ	X	Base excision repair	–
μ	X	Nonhomologous end joining	10^{-1}
σ	X	Sister chromatid cohesion	–
TDT	X	Antigen receptor diversity	–
η	Y	Bypass synthesis	10^{-2}
ι	Y	Bypass synthesis	10^{-1}
κ	Y	Bypass synthesis	10^{-2}
Rev1L	Y	Deoxycytidyl transferase	–

Table 1. Families of DNA Polymerases and their error frequencies[3].

replication, the normal DNA polymerase allows replication up to the DNA lesion, but cannot bypass it. Ideally, these adducts are removed by NER while cell cycle transit is arrested during the DNA damage response (DDR). However, if the adduct is not removed before DNA synthesis resumes, the stalled DNA polymerase III will be replaced with Pol-η (Fig.3), and Pol-η will insert bases in the growing daughter strand opposite these damaged bases, risking the introduction of point mutations, before normal DNA replication resumes. These TLS processes are used as a type of survival mechanism, protecting the cell from UV-induced apoptosis. Transcription-coupled NER (TC-NER) is the type of DNA damage repair mechanism required for removal of bulky base adducts that block transcription on the template strand of active genes. Global genomic NER (GG-NER) removes UV-induced lesions from the rest of the genome

Fig. 3. Trans-lesion Synthesis. The steps of TLS are shown with Pol-η[8].

9

and is independent of ongoing transcription[11].

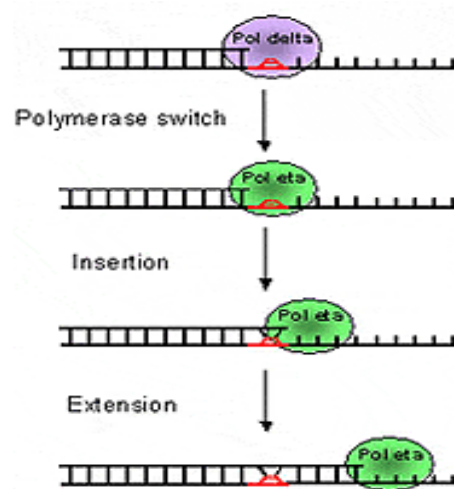On earth, we are exposed to far more ultraviolet-B (UV-B, 280-315 nm) and ultraviolet-A (UV-A, 315-400 nm) radiation than ultraviolet C (UV-C, 100-280 nm). Per joule of irradiation, UV-B causes more damage to DNA than does UV-A. Although UV-C is the most damaging of the three, negligible amounts of solar UV-C radiation penetrate the atmospheric ozone layer. Most experiments relating to UV-induced DNA damage are done using UV-C, simply because UV-C is more efficient in causing CPD and (6-4) PP adducts in the DNA.

Hutchinson-Gilford Progeria Syndrome (HGPS) cells display a rate of aging up to ten times that of normal human fibroblasts. One feature of HGPS cells is a more rapid accumulation of DNA damage (strand breaks) as they age during repeated passage in culture. This premature aging seems to be related mostly to inefficient DNA repair, as shown in several other premature aging disorders, which all have some deficiency in repairing DNA.   When the genome is damaged, normal BJ fibroblasts arrest their cell cycle transit for DNA repair before progressing through replication and mitosis. We might expect that these aging HGPS cells would exhibit a decreased ability to repair DNA damage and, thus, be delayed in continuing through the cell cycle. The mutation that causes HGPS occurs at base position 1824 of the LMNA gene, replacing cytosine with thymine. Rather than causing an amino acid change in the protein, this mutation causes a defect in the splicing maturation of prelamin A to lamin A mRNA. This leads to an accumulation of progerin, a shortened and farnesylated form of the lamin A protein[5]. Progerin causes abnormal chromatin and lobulated nuclei, leading to premature aging with an accumulation of DNA damage. Progerin and DNA damage also accumulate in normal individuals but is detectable only at advanced age[5]. Thus, HGPS cells serve as a useful model for normal human aging. The relative sensitivity of premature aging HGPS cells to UV-B radiation is unknown.

Pol-η is a protein of interest for several reasons. In previous studies, UV exposure caused transient stabilization of Rad30, the homolog of Pol-η in yeast, which caused accumulation of Rad30 in the cell. This over-expression of Rad30 increased the frequency of spontaneous mutations[2]. This study suggested that an overexpression of Pol-η could result in a further accumulation of mutations in addition to those already imposed by the premature aging and the UV irradiation. Other studies examined Xeroderma Pigmentosum-Variant V (XP-V), which have normal NER, but are defective in DNA replication following UV exposure. A deficiency of Pol-

η causes XP-V, with extreme sunlight sensitivity and a high rate of skin cancer. The status of Pol-η in HGPS cells of different ages remains unknown. The subcellular location and levels of this protein may elucidate why HGPS cells display inefficiency in DNA repair.

The second protein of interest is the DNA-Damage Binding Protein (DDB). This protein consists of two subunits: DDB1 and DDB2, with molecular masses of 127 and 48 kDa (also known as p127 and p48, respectively). Its activity requires the formation of the heterodimeric complex. Its main role is to find DNA damage sites and recruit repair proteins to them. It is activated in response to DNA damage and is then degraded once the damage sites are found and NER is initiated. Several studies have found mutations in DDB2 in *Xeroderma Pigmentosum-E* patients, but not mutations in DDB-1. These mutations in DDB2 resulted in a loss of heterodimeric formation, generating a DDB deficiency. DDB is specifically involved in GG-NER, especially in the repair of CPDs, and in the initiation step of NER. The mutations in DDB2 disrupted the nuclear localization of DDB1, a necessary event for DDB function. In DDB mutation variants in HeLa cells irradiated with 30 J/m^2, both subunits were shown to be dominant negative inhibitors of DNA repair, creating a deficiency in the heterodimeric complex formation. Mutations in either subunit inhibited repair of CPDs. The mutations inhibited the activity of normal DDB2 expressed from the endogenous genes in these HeLa cells[6]. In other studies, DDB2 was shown to be up-regulated by the p53 tumor suppressor protein. P53 protects cells exposed to UV at moderate levels, but induces apoptosis at high levels. After UV exposure, p53 accumulates in nuclei and regulates the activity of target genes like DDB2. If cells can't repair the damage, p53 accumulates in nuclei and cause apoptosis at lower levels of UV than normal[6]. As described previously, XP-E shows mutations in DDB2, and since DDB2 is required *in vivo* for GG-NER of CPD's and since the heterotrimeric active complex, DDB1-Cul4A-DDB2, formed at the damaged site is required to recruit other NER proteins to fix UV lesions, a deficiency of DDB2 would result in inadequate DNA repair[7]. This highlights DDB2 as another protein of interest since the relative levels of this protein also are unknown in HGPS, and could lend further insight into the mechanisms of their DNA damage repair.

In preliminary studies, we observed that HGPS cells appear to repair the DNA damage induced by ultraviolet light (UV-C) and resume cell cycle transit with short-term viability equal to normal BJ fibroblasts. Determining the relative sensitivity on a cellular viability level of HGPS and of BJ cell lines to UV-B and UV-C will be one focus of this study.

The specific aims of this research are to illuminate underlying mechanisms that either accelerate or slow the aging process in HGPS patients. Since the children affected with this syndrome have a normal mental capacity but a rapidly aging body, most are fully aware of their own condition early on, dying in their pre-teens. Thus, this syndrome is especially heartbreaking. Understanding the processes involved in DNA repair and the relevant differences between HGPS and BJ cells holds promise in better understanding this syndrome and perhaps in pointing towards treatments for HGPS patients. In addition, understanding underlying mechanisms of aging, using HGPS as a model system, can further promote our understanding of the normal aging process, factors that affect it, and ways to treat or delay it.

In these studies, it is hypothesized that the normal BJ fibroblasts will exhibit a faster rate of DNA repair and a higher level of cell viability after exposure to ultraviolet-B radiation than would be observed with the HGPS fibroblasts, and that these differences would be greater as the HGPS cells age in culture. When exposed to UV-C, it is hypothesized that young fibroblasts should repair their DNA and resume cell cycle progression sooner than older fibroblasts. Since older HGPS cells tend to accumulate damage and repair less efficiently, they are expected to take longer to repair their UV-damaged DNA than BJ or younger HGPS cells. The final hypothesis is that, with increasing amounts of UV irradiation, an increase in the amount of Pol-η and DDB2 would be seen, and, because older cells take longer to repair and enter replication, the Pol-η and DDB2 in HGPS is expected to be less effective than in normal fibroblasts.

Chapter 2. METHODS AND MATERIALS

Measuring Cellular Viability by Tracking Metabolic Activity Following UV-B Irradiation

Cell Culture

The purpose of these initial studies was to measure the effect of UV-B on cell cycle progression in normal *vs.* HGPS cells. To achieve this goal, BJ and HGPS cell cultures were established, the cells were exposed to UV-B, then analyzed after a set recovery time with the Cell-Titer Blue Viability Assay (Promega). This assay is designed to determine viability by recording the metabolic activity of the cells in the culture dish. HGPS cell stocks were grown in T-25 flasks with EMEM containing 15% FBS + 1% Penicillin/Streptomycin antibiotics; BJ cell stocks were grown in T-25 flasks with EMEM containing 10% FBS + 1% Penicillin/Streptomycin antibiotics at 37ºC in humidified air containing 5% CO_2. While rapidly growing (70-80% confluency), the cells were harvested and placed into a 96-well CellStar, black microtiter plate with clear bottoms, with $6x10^3$ cells plated into each well. The microtiter plate then was incubated at 37ºC for 24 hours.

Fig. 4. **Cell-Titer Blue Viability Assay (Promega).** This fluorometric assay measures the conversion of resazurin to resorufin by metabolic enzymes in live cells. Resorufin production is measured as an increase in fluorescence at 590 nm.

UV-B Irradiation

The media was removed and the wells were washed twice with 1x Phosphate-Buffered Saline (PBS, In 500 ml: 0.0168 moles monobasic sodium phosphate, 0.072 moles dibasic sodium phosphate, 4.5g NaCl). The cells were exposed to UV-B while covered with 50 µl of PBS. The exposure levels were as follows: 0, 4, 8, 12, 24, and 50 J/m^2. The PBS was removed following the UV-B exposure and fresh media was added to the wells. The plate was incubated at 37ºC and the cells were allowed to recover for 72 hours.

Cell Viability Assay

Following the recovery period, 10 µl of the Cell-Titer Blue Reagent was added to each well and incubated at 37ºC for 90 minutes. The fluorescence (Fig. 4) was recorded using a spectrofluorimeter with $\lambda_{ex} = 560$ nm and $\lambda_{em} = 590$ nm.

Measuring Cellular Viability by Metabolic Activity Following UV-C Irradiation

Cell Culture

We also determined the effects of UV-C exposure on cell cycle progression. To do this, cultures of BJ and HGPS cells were exposed to UV-C, then analyzed after a set recovery time with the Cell-Titer Blue Viability Assay. As describe in the preceding section, this assay tracks the viability by recording the metabolic activity of the cells in the plate. HGPS and BJ cell stocks were grown in T-25 flasks as described above. While rapidly growing, the cells were harvested and placed into a 96-well CellStar, black microtiter plate with clear bottoms at $6x10^3$ cells per well. The microtiter plate was then incubated at 37ºC for 24 hours.

UV-C Exposure

The media was then removed and the wells were washed twice with 1x PBS. The cells were exposed to UV-C in 50 µl of PBS. The exposure levels were as follows: 0, 5, 10, 20, and 40 J/m^2. The PBS was removed following the UV-C exposure and fresh media was added to the wells. The plate was incubated at 37ºC and the cells were allowed to recover for 72 hours.
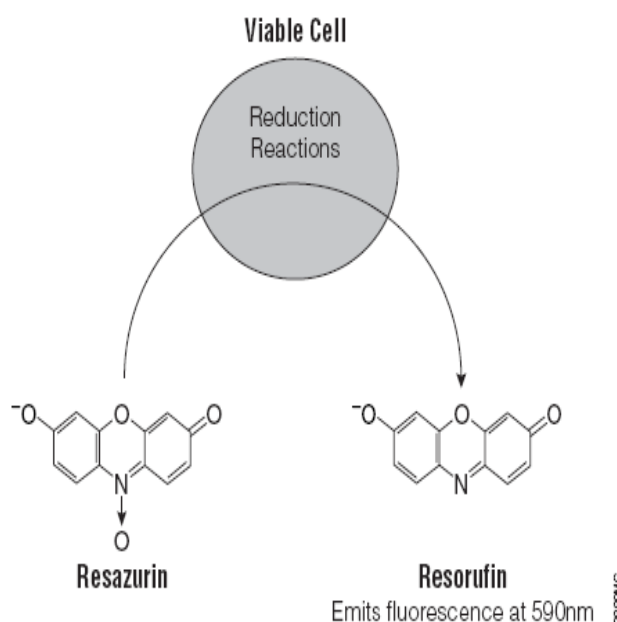
Cell Viability Assay

Following the recovery period, 10 µl of the Cell-Titer Blue Reagent was added to each well and incubated at 37ºC for 90 minutes. The fluorescence was recorded using a spectrofluorimeter with $\lambda_{ex} = 560$ nm and $\lambda_{em} = 590$ nm.

Tracking cell growth by measuring DNA content of cultures

Sybr Green Analysis of DNA Content

Total cellular DNA was measured to quantify the total number of cells attached to the plate that may be metabolically less active due to repair processes but still viable and missed by the

Cell-Titer Blue assay.

Following the removal of the Cell-Titer Blue reagent, the wells were washed twice with PBS. Then, 15 µl of a mixture containing 5% formamide/2 µg/ml Protease K/33.3 mM EDTA was added to each well to lyse the cells and release the DNA into solution by incubation at room temperature for one hour. Sybr Green was obtained as a 10,000X stock (Cambrix Biosciences, Cat. # 50513) and the working stock contained a 1.08x concentration of Sybr Green in 10 mM Tris-HCl with 1 mM EDTA, pH 8.4 (TE). 185 µl of this Sybr Green was added to each well and the fluorescence read on a spectrofluorimeter at $\lambda_{ex} = 485$ nm and $\lambda_{em} = 524$ nm, with $\lambda_{cutoff} = 515$ nm.

Measuring the Effect of UV-C on Long-Term Cell Growth and Viability

Cell Culture

Do the short-terms effects of UV radiation revealed by the above studies continue over a longer recovery period? To answer this question, cultures of BJ and HGPS cells were exposed to UV-C, then analyzed after increasing recovery times with the Cell-Titer Blue Viability   HGPS and BJ cell stocks were grown in T-25 flasks with as described above. A549 cells were grown in a T-25 flask with DMEM + 10% FBS and antibiotics. Rapidly growing primary cells at different ages were harvested and seeded into three Costar 96-well microtiter Stripwell plates with low evaporation lids (Corning. Lot#11610020; C# 9102) at $6x10^3$ cells per well. The microtiter plates then were incubated at 37ºC for 24 hours.

UV-C Exposure

The media was removed and the wells were rinsed twice with PBS. The cells in two of the microtiter plates were exposed to 20 J/m^2 UV-C in 50 µl of PBS. The third plate was used as a control without UV irradiation. The PBS was removed following the UV-C exposure and fresh media was added to the wells. The plate was incubated at 37ºC and the sets of cells were allowed to recover for the following number of days: 0, 3, 4, 5, 6, 8, 10, 12 and 14.

Cell-Viability and Sybr Green Assays

Following the end of each recovery period, the corresponding strip wells were removed and placed into an empty rack. Then 10 µl of the Cell-Titer Blue Reagent was added to each well

and incubated at 37ºC for 90 minutes. The fluorescence was recorded using a spectrofluorimeter with λ_{ex} = 560 nm and λ_{em} = 590 nm. Following the fluorometric reading, the wells were covered with parafilm and placed at 4ºC until the entire plate was read after fourteen days. The same Sybr Green protocol for DNA determination as described above was followed to determine the amount of DNA in each of the wells.

Statistical Analysis of the Cell-Viability Data

The fluorescence values were plotted on a graph in Microsoft Excel and linear regression analysis of the data was performed for each cell type. To compare the linear regression lines of the different cell types, the slopes were evaluated to determine similarity by the ANCOVA method. A 'p' value is given and if it is greater than 0.05, the slopes are deemed not to be significantly different, which is interpreted as no significant difference in cell viability between the cell types.

Determining UV-C's effect on the Proteins of HGPS and BJ in Two Cell Fractions: Nucleoplasm and Chromatin

Do the cellular levels of specific DNA repair-associated proteins change during the DNA damage response (DDR) period.   To check for such differences cultures of BJ and HGPS cells were exposed to UV-C, then analyzed by SDS-Page/Western Blotting after a set recovery time. HGPS and BJ cell stocks were grown as described above. Three T-25 culture flasks at approximately 70% confluency for each cell type were harvested and $5x10^5$ cells were placed in 100 mm culture dishes and incubated at 37ºC for 24 hours.

The media then was removed and the plates rinsed twice with PBS. The cells were exposed to UV-C (254 nm) in 2 ml of PBS at 0, 10, 20 J/m^2. The PBS was removed following the UV-C exposure and replaced with fresh media. The dishes were incubated at 37ºC and the cells were allowed to recover for four days (96 hours).

Cell Fractionation

The dishes were washed with PBS and the cells scraped into centrifuge tubes. The tubes were spun at 500xG for ten minutes at 4ºC, and the pellet resuspended in 500 μl Pol-η Lysis Buffer

(100 mM Tris-HCl pH 6.8, 300 mM sucrose, 100 mM NaCl, 3 mM $MgCl_2$, 1 mM EGTA) and incubated at 4ºC for thirty minutes with rotation. The tubes then were spun at 5000xG for fifteen minutes at 4ºC and the supernatant transferred to a tube titled "Cytoplasm-1." The pellet was resuspended in 500 µl Pol-η Lysis Buffer and incubated at 4ºC for ten minutes, then the tubes were spun at 2,000xG at 4ºC for fifteen minutes. The supernatant was again transferred, and the recipient tube was titled "Cytoplasm-2." The pellet was resuspended in 500 µl High Salt Pol-η Lysis Buffer the (Pol-η Lysis Buffer described above plus NaCl added to a final concentration of 420 mM), incubated at 4ºC with rotation for twenty minutes before spinning at 2,000xG for fifteen minutes at 4ºC. The supernatant was transferred to another tube titled "Nucleoplasm." The final pellet was brought up in 500 µl High Salt Pol-η Lysis Buffer supplemented with 5 µl of 1M $MgCl_2$ and 10 µl of 20 µg/ml DNase I before incubation at 4ºC for twenty minutes to digest the DNA. This tube was labeled "Chromatin." The labels on the tubes indicated which subcellular fraction they contained.

TCA Precipitation

To concentrate the proteins xx µl of 100% trichloroacetic acid (TCA) was added to each fraction and incubated at 4ºC for ten minutes, spun at 5,000xG for ten minutes, and the pellet was rinsed three times with 100% acetone. The final pellets, after being air dried, were dissolved in 67 µl Pol-η Lysis Buffer and 25 µl of 2.5x Urea Sample Loading Buffer (USLB, the 2.5X SLB described in the Molecular Cloning Manual[10] containing 10M urea). The samples were boiled for ten minutes and then immediately frozen at -20ºC.

Western Blotting

A 10% polyacrylamide gel containing SDS (SDS-Page gel) was prepared[10] with a fifteen slot comb in a Bio-Rad Protean System apparatus; 30 µl of sample was loaded per well. The Chromatin and Nucleoplasm fractions were run on separate gels for 55 minutes at 150 volts, with the current starting at 50 mA and ending at 20 mA. The molecular weight standard was composed of 49.2 µl 1x USLB diluted in Pol-η Lysis Buffer, 10 µl EZ-Run Protein Standard (Prestained, from Fisher Bioreagents, BP3603-500), and 0.8 µl MagicMark XP (Western Protein Standard, Invitrogen, C# LC5602); 30 µl of the standard was loaded per well. After electrophoresis the Western transfer was done using Invitrogen Xcell II Blot Module (C#

EI9051- Version 1) for 70 minutes at 30 volts onto either nitrocellulose or polyvinylidene difluoride (PVDF) membranes. The membranes were blocked overnight in 5% BSA in TBST (Tris-buffered Saline + 0.05% Tween-20).   The membranes were probed with the following primary antibodies obtained from Santa Cruz Biotechnology Company: rabbit anti-Pol H (SC-5592) and rabbit anti-DDB2 (SC-25368).

Table 2. Organization of SDS-Page gels for the chromatin and nucleoplasm fractions.					
Chromatin Fraction			Nucleoplasm Fraction		
Well	Sample	UV-C J/m^2	Well	Sample	UV-C J/m^2
1	Young BJ (yB)*	0	1	yB	0
2	Middle-age BJ (maB)*	0	2	yB	20
3	yB	10	3	yB	10
4	yB	20	4	maB	10
5	maB	20	5	maB	20
6	Protein Markers	-	6	Protein Markers	-
7	Young HGPS (yH)*	0	7	yH	0
8	Middle-age HJPS (maH)*	0	8	maH	0
9	Old HGPS (oH)*	0	9	oH	0
10	yH	10	10	yH	10
11	maH	10	11	maH	10
12	oH	10	12	oH	10
13	yH	20	13	oH	20
14	yH	20	14	maH	20
15	oH	20	15	oH	20

*These abbreviations will be used in the results section of Figs. 9 and 12.

The protocol for probing included adding 4 mL of appropriately diluted (1/200 dilution for SCBT primary antibodies) antibody and incubating at room temperature for one hour or overnight at 4ºC in a sealed plastic bag. Following the incubation, the membranes were washed with15 ml TBST on a rocker three times for ten minutes each at room temperature. Four ml of appropriately diluted secondary antibody then was added to each membrane in a separate sealed

18

plastic bag for 45 minutes to one hour at room temperature. The membranes again were washed on a rocker three times for ten minutes each in TBST. The membrane was soaked in Invitrogen Novex ECL chemiluminescent substrates (catalog#WP2005) and the chemiluminescence image captured using the Fuji LSR-4000 Imager and analyzed with the Multigauge Image Processing software from Fuji.

Measurement of Viability in Response to UV Irradiation

The first results determine the cell viability of the two cell types using two separate methods, the Cell-Titer Blue Viability Assay and the Sybr Green assay. The first gives a reading that uses metabolic activity as the indicator for cell viability. The second gives a reading that uses DNA content as an indicator for cell number and, thus, viability. In Figs. 5 and 6, cells were exposed to UV-B and allowed a 72 hour recovery prior to either assay. The fluorescence was then plotted and further analyzed by linear regression analysis and ANCOVA. ANCOVA yielded the values $F = 0.0608$, DFn = 1, DFd = 6, $P = 0.8135$, indicating there is no significant difference between the recovery of BJ and HGPS after a three-day period (Fig. 5).

Figure 5. *Measuring Cellular Viability in Response to UV-B Irradiation*
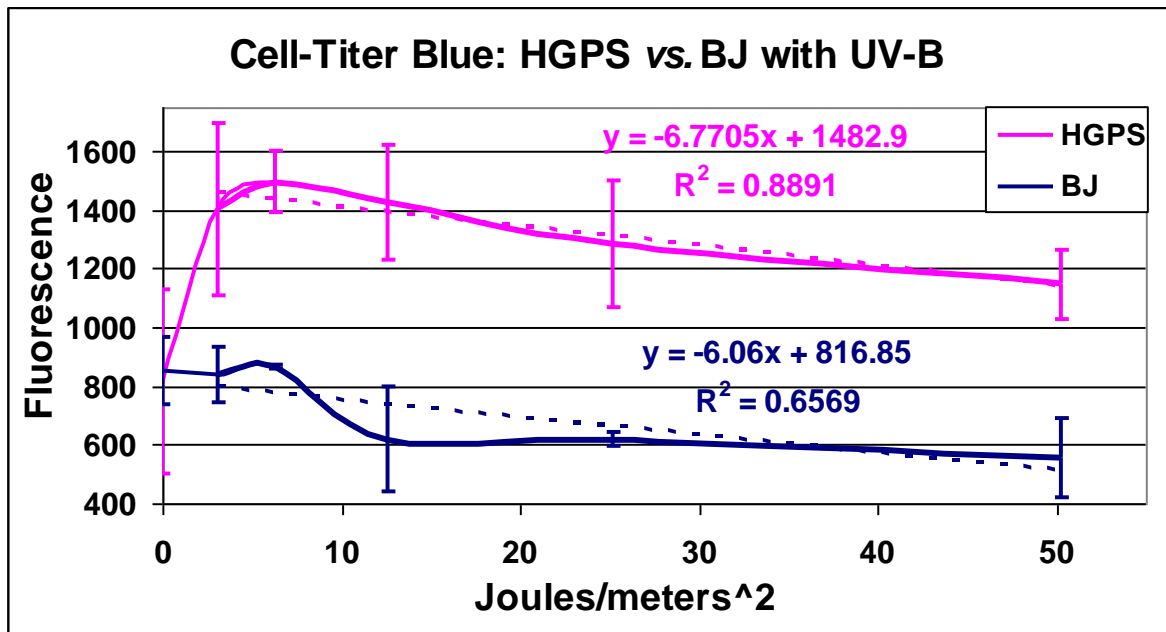
Figure 5. Measuring Differences in Viability of BJ and HGPS in Response to UV-B Exposure. Cells were cultured in a 96-well microtiter plate and exposed to varied levels of UV-B after 24 hours. Following a 72-hour recovery, the Cell-Titer Blue Viability Assay was performed to determine whether a difference in viability could be found. A higher amount of fluorescence indicates a greater number of cells converting resazurin to the fluorescing product resorufin.The linear regression lines were compared by an ANCOVA statistical analysis which generated the values $F = 0.0608$, DFn = 1, DFd = 6, $P = 0.8135$.

The second set of data is that of the Sybr Green assay (Fig. 6). The reason behind following up the Cell-Titer Blue assay with this was to ensure that viable cells with reduced metabolic activity were also measured. The cells were lysed using in a formamide-EDTA solution

containing protease K to hydrolyze cellular protein. This allowed for the most optimal results for Sybr Green analysis. The fluorescence was then plotted and further analyzed by linear regression analysis and ANCOVA. ANCOVA yielded the values F = 0.0608, DFn = 1, DFd = 6, P = 0.8135, once again indicating no significant difference between the recovery of BJ and HGPS after a three-day recovery (Fig. 6). This not only shows that no difference was detected between the two cell types after a three day recovery from UV-B radiation, but also that the Cell-Titer Blue and Sybr Green assays yield the same results.

Fig. 6. Measuring DNA Content in Response to UV-B Irradiation
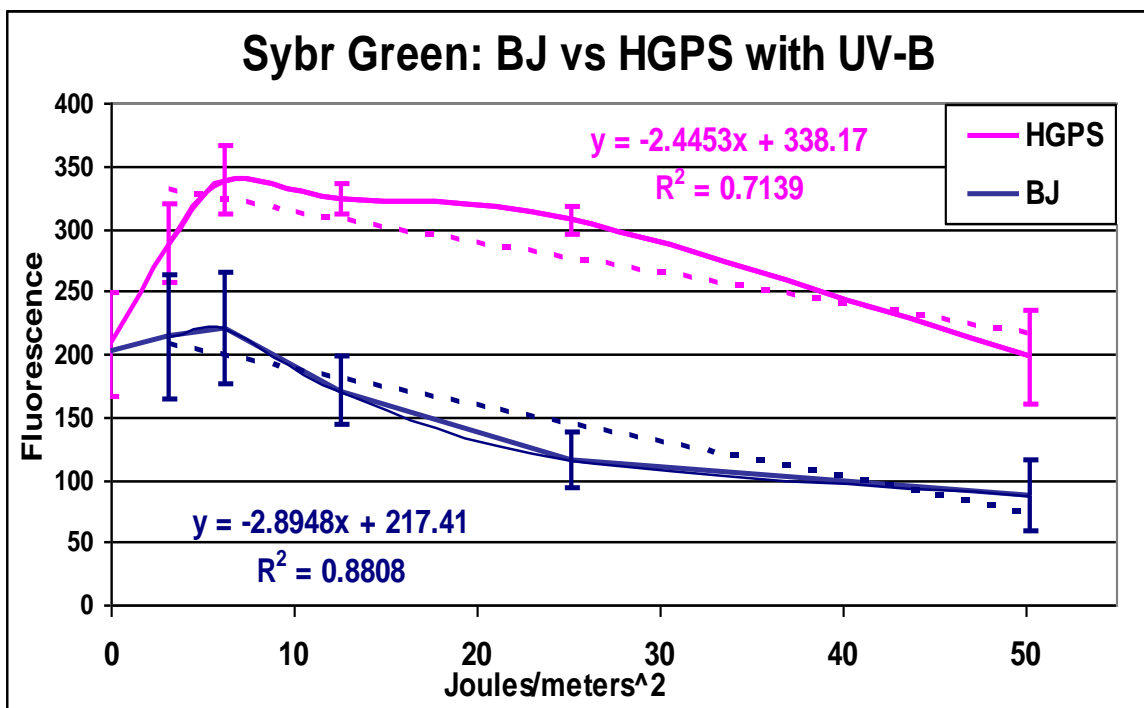
Figure 6. **Measuring DNA Content as an Indicator of Cell Viability in Response to UV-B**

Irradiation. Following the Cell-Titer Blue Assay, cellular DNA was released with a formamide lysis-protease and stained with Sybr Green. As described above, ANCOVA was used to determine a if there was significant difference between the slopes (F = 0.1717, DFn = 1, DFd = 6, P = 0.693).

Similar methods were employed to compare the viability of BJ *vs*. HGPS cells exposed to UV-C after a three-day recovery. These data are shown in Figure 7. The data points for the first two exposures were outliers and were excluded from further analysis.   The ANCOVA values are F = 0.3166, DFn = 1, DFd = 4, P = 0.6037. The high p-value indicates that the recovery rates are

not statistically different for the two cell types after a three-day recovery, even at a more intense UV-C radiation levels.

Figure 7. Measuring Cellular Viability in Response to UV-C Irradiation
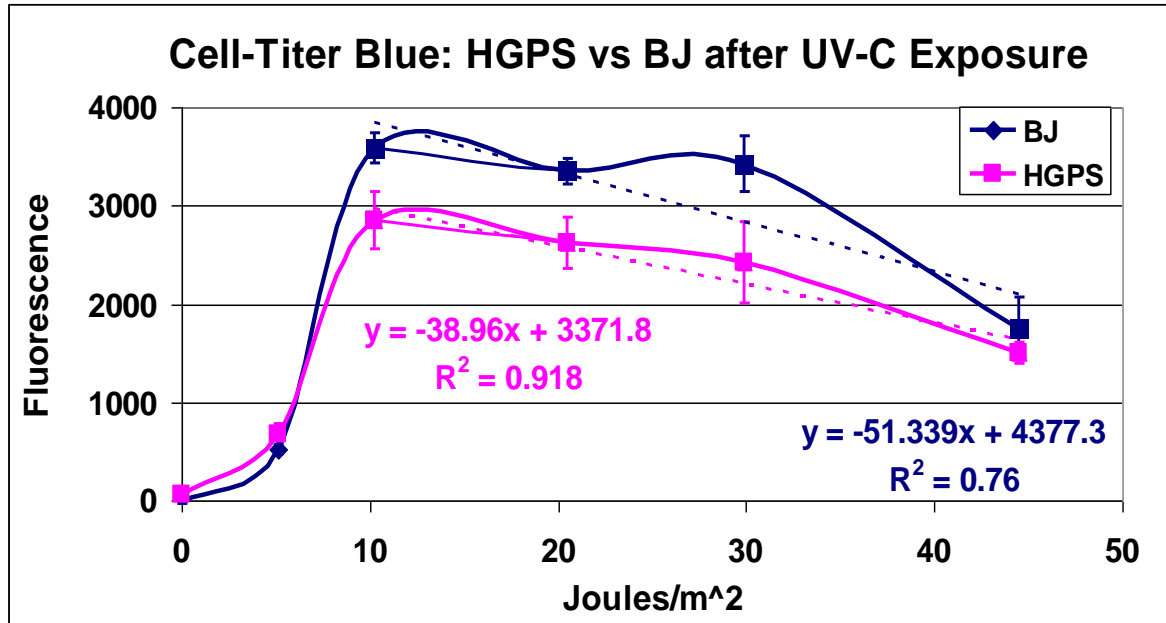
Figure 7. Determining Cellular Viability in Response to Varying Levels of UV-C in HGPS and BJ. The same method was repeated here as described above, however varying levels of UV-C were used and followed with a three-day recovery. Once again, ANCOVA and linear regression analyses were used, generating the values $F = 0.3166$, $DFn = 1$, $DFd = 4$, $P = 0.6037$.

Do the recovery patterns change when monitored over a longer recovery period? To resolve this question, BJ and HGPS cells were irradiated and allowed to recover for periods up to 15 days to determine if a difference appeared after a long-term recovery. The same type of assay was utilized; however, strip-well plates were employed to prevent contamination and variability from the assay with 20 J/m^2 of UV-C. In addition to BJ and HGPS, A549 cells were used as a positive control. These are a lung carcinoma cell line and are shown to repair DNA and to divide quicker than either BJ or HGPS (Fig. 8). BJ cells were observed to recover more quickly than HGPS cells; both ages of HGPS cells have difficulty repairing and then dividing over the long-term.

Figure 8. Determination of the Effect of UV-C on Long-Term Cell Growth and Viability
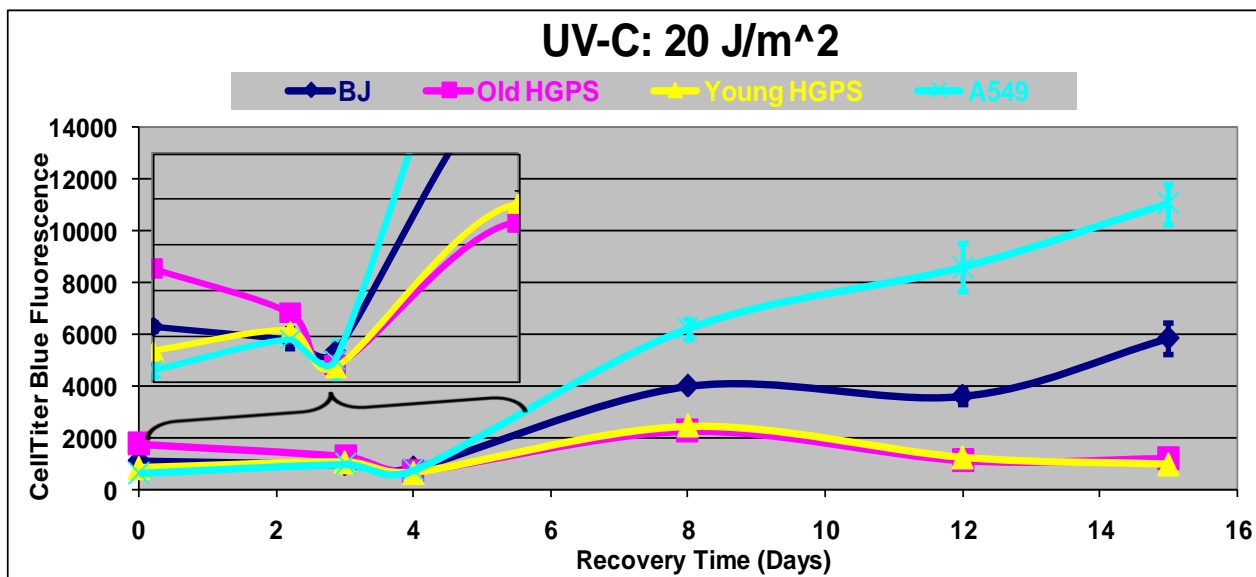
Figure 8. Measurement of Cell Viability and Long-term Growth in Response to UV-C Irradiation. Cells were seeded in a 96-well strip-well plate. After 24 hours, the initial time point was read using the Cell-Titer Blue assay, then the cells were exposed to 20 J/m^2 UV-C. Strip wells were used and discarded after each time point to prevent variability from the assays on sample readings. Recovery of cell growth is seen to occur between the three and four day time points. A549 cells were used as a positive growth control.

Measurement of Protein Amounts in Response to UV Irradiation

The status of Pol-η and DDB2 proteins were assayed using Western blotting analysis. Cells were grown in culture dishes, exposed to varying levels of UV-C, and allowed to recover for either 2.5 or 4 days. Then, cells were harvested and separated into subcellular components and the proteins concentrated by TCA precipitation. After separation by SDS-Page electrophoresis, the proteins were blotted onto a PVDF or nitrocellulose membrane for probing with antibodies specific for Pol-η or DDB2 proteins.

The subnuclear distribution of Pol-η protein between the chromatin and nucleoplasm was investigated by western blotting of the respective fractions of HGPS and BJ cells after a four-day recovery from UV-C exposure. The analysis of the chromatin-bound Pol-η and the nucleoplasm-associated Pol-η are illustrated in Figure 9 Panels A and B, respectively. The TLS enzyme is

bound to chromatin in both BJ and HGPS cells. In the nucleoplasm fraction, Pol H only appears in the HGPS cells, though the amount of nucleoplasmic enzyme varies depending on culture age of the cells and level of UV-C irradiation.

Panel A:

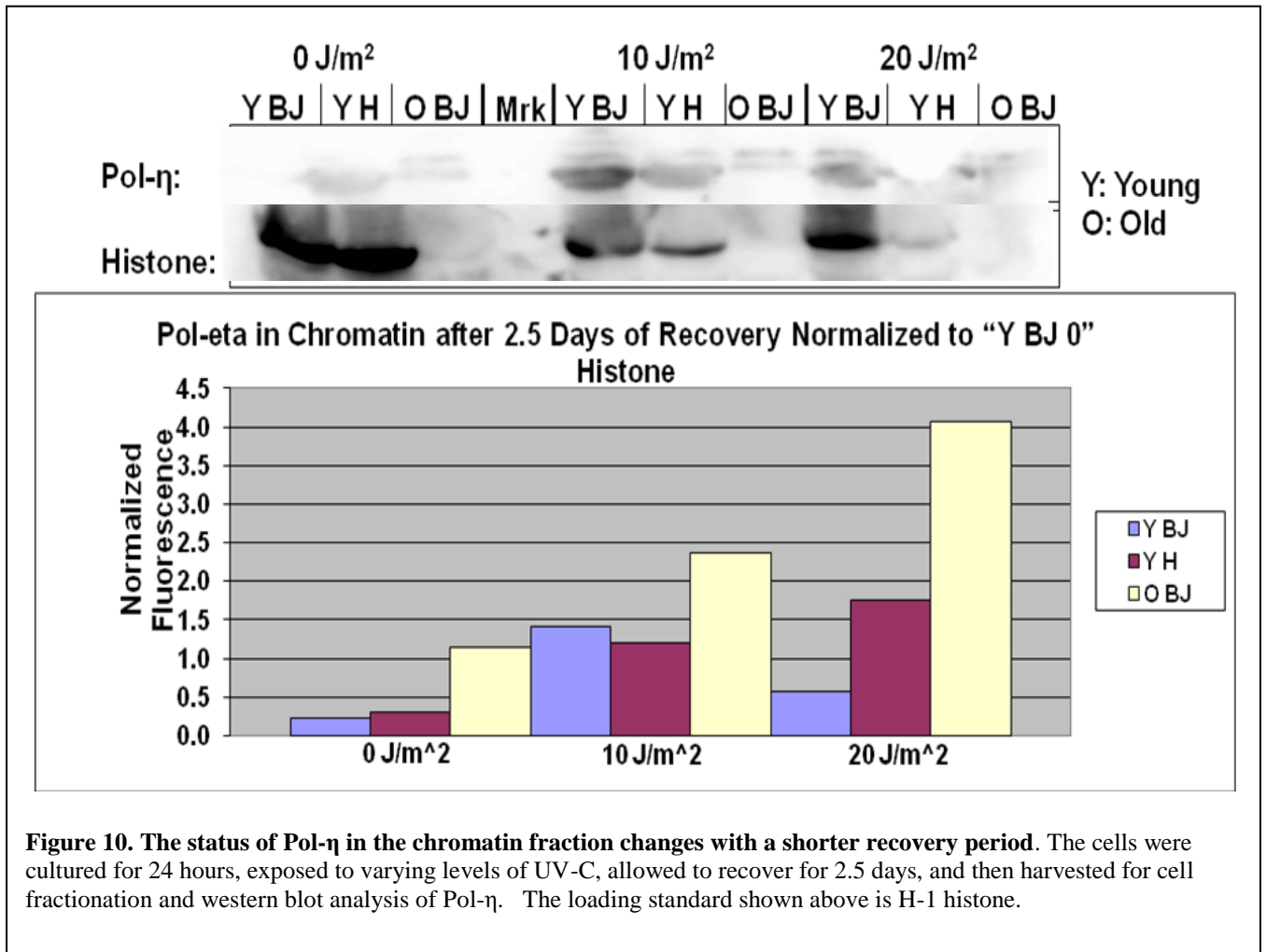| Age, cell type	yB		maB	yB	yB	maB		yH	maH	oH	yH	maH	oH	yH	maH	oH
UV-C (J/m^2)		0			10				0			10			20	.
Lane	1	2	3	4	5	6	7	8	9	10	11	12	13	14	15

PolH

Figure 9. **Pol-η distribution between subnuclear fractions differs between BJ and HGPS cells.** Cells were cultured for twenty-four hours, exposed to 20 J/m² UV-C, allowed to recover for four days, and then harvested for cell fractionation. The distribution of Pol-η in the nuclear fractions is shown in Panel A and in the nucleoplasmic fraction in panel B. The text above each panel indicates the age and cell type for each sample, the UV-C exposure in J/m² and the lane number corresponding to the gel loading sequence defined in Table 2.

Panel B:

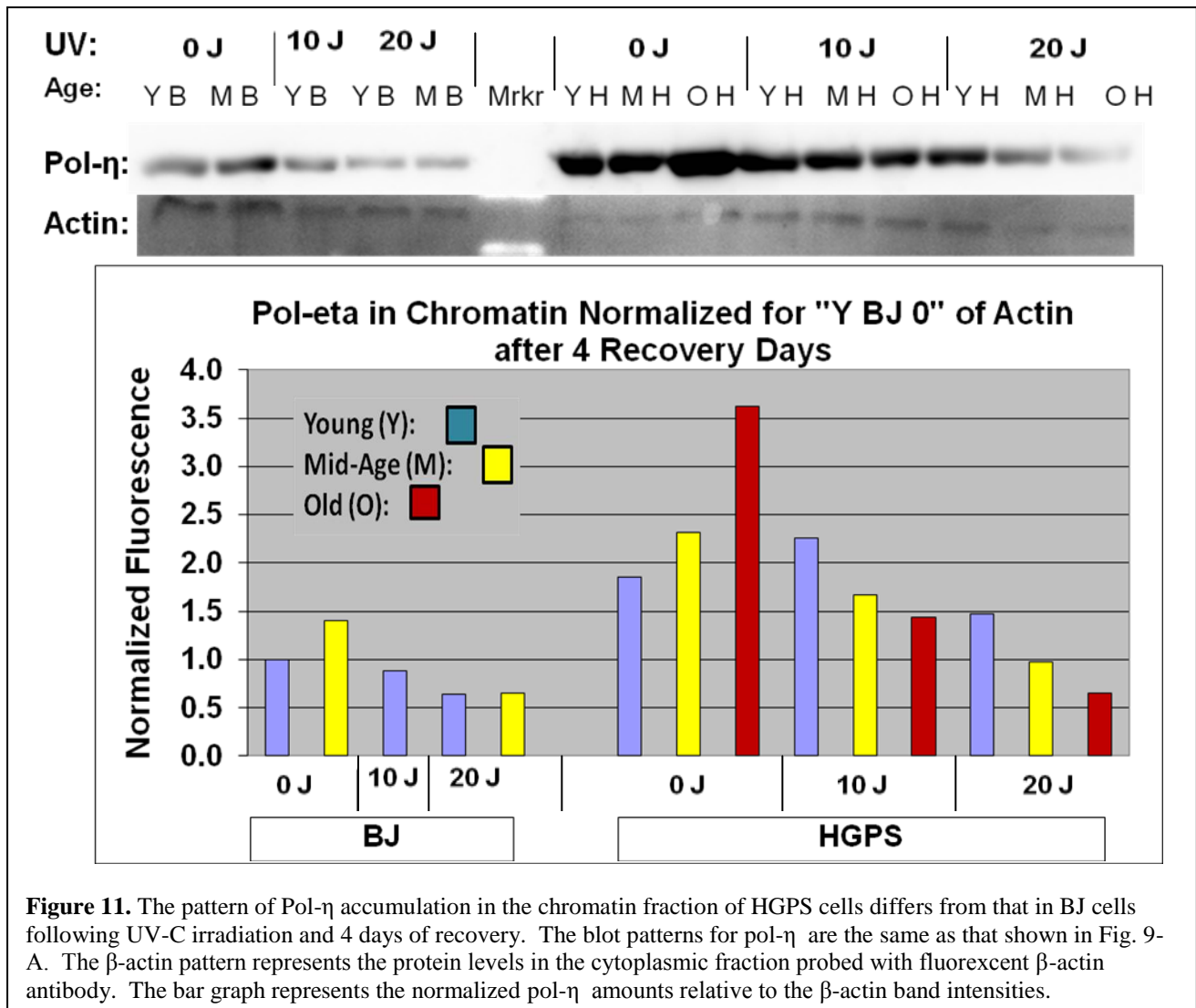| yB 0	yB 20	yB 10	maB 10	maB 20	Mr kr	yH 0	ma H 0	oH 0	yH 10	ma H 10	oH 10	yH 20	ma H 20	oH 20

PolH

Pol-η is involved in DNA replication once cell cycle transits restarts after the DNA damage response to UV-induced bulky base lesions. Thus, if the repair phase takes longer, restart of cycle transit would be delayed as would the resumption of DNA replication. Thus, do the amounts and distributions of Pol-η between chromatin and nucleoplasm depend on the recovery

period? To resolve this question another experiment was performed to analyze the amount and subnuclear distribution of Pol-η with a recovery time of 2.5 days instead of four days. The data in Figure 10 show a relationship between the amount of UV-C and the amount of Pol-η present in the chromatin fraction in young and old BJ and in young HGPS.

Figure 10. The status of Pol-η in the chromatin fraction changes with a shorter recovery period. The cells were cultured for 24 hours, exposed to varying levels of UV-C, allowed to recover for 2.5 days, and then harvested for cell fractionation and western blot analysis of Pol-η.   The loading standard shown above is H-1 histone.

In order to look at the effect of UV on Pol-η levels after a longer recovery time, the assays were completed on cells after a four-day recovery. The Pol-η levels displayed in this western analysis are displayed below in numeric graphical format in Figure 11. This graph is made using the actin of the cytoplasm fraction as the baseline values to standardize for variation in protein loading. These values are comparable since they come from the same cells, went through the same fractionation and precipitation, and were diluted the same when being loaded onto the gel. An increase in the amount of Pol-η is not seen as the amount of UV is increased (Fig. 11). The

irradiated cells were observed to resume growth at 4 days into recovery (Fig. 8), indicating that these cells had reached a decision point whether the damage was extensive enough to enter apoptosis or whether it was repairable. BJ cells have fairly level amounts of Pol-η regardless of UV exposure amounts as shown below, indicating that either senescent cells or those that have already repaired a large majority of the damage, therefore no longer needing the Pol-η. Mid-age and old-age HGPS cells show a decreasing amount of Pol-η as the UV dose increases. These findings indicate that HGPS cells becoming senescent, preparing for apoptosis. At 0 J/m^2, old HGPS cells have the highest level of Pol-η. This is consistent with the concept that accumulation of DNA damage in HGPS as they age stimulates Pol-η buildup, perhaps in addition to that induced by UV-damage. This indicates a difference between BJ and HGPS after a recovery of four days.

Figure 11. The pattern of Pol-η accumulation in the chromatin fraction of HGPS cells differs from that in BJ cells following UV-C irradiation and 4 days of recovery. The blot patterns for pol-η are the same as that shown in Fig. 9-A. The β-actin pattern represents the protein levels in the cytoplasmic fraction probed with fluorexcent β-actin antibody. The bar graph represents the normalized pol-η amounts relative to the β-actin band intensities.

DDB2 is part of the early response system for recognition and repair of UV-damaged DNA. To determine whether there are differences in DDB2 between BJ and HGPS cells and the influence of UV irradiation on the status of this protein the amounts of DDB-2 present in the cells following a four-day recovery was determined by re-probing the western blots used for Pol-η measurements. As shown in Fig. 12, DDB-2 was not found in the chromatin nor the nucleoplasm fractions of either cell line. As a control, a western blot of UV-irradiated HeLa cells nuclei and cytoplasmic fractions with a three-hour recovery was probed to verify the activity of the DDB2 antibody.

Panel A:

Lane:	1	2	3	4	5	6	7	8	9	10	11	12	13	14	15
	yB	maB	yB	yB	maB		yH	maH	oH	yH	maH	oH	yH	maH	oH
Sample:	0	0	10	20	20	Mrkr	0	0	0	10	10	10	20	20	20

DDB2

Panel B:

yB	yB	yB	maB	maB	Mr	yH	ma H	oH	yH	ma H	oH	yH	ma H	oH
0	20	10	10	20	kr	0	0	0	10	10	10	20	20	20

DDB2

Panel C:

	Cytosol				Nucleus			
	SiRNA control		SiRNA MK2		SiRNA control		SiRNA MK2	
UV	0J	20J	0J	20J	0J	20J	0J	20J

DDB2

Figure 12. **Measuring the amounts of DDB2 in varied ages, cellular fractions, and UV-C dosage levels in BJ and HGPS.** Refer to Table 2 for the figure legends. Panel A: Chromatin Fraction Comparison with DDB2 Levels. The same methods were used as described above. Panel B shows the nucleoplasm fraction comparison of DDB2 levels. The same methods were used as described above, but using the nucleoplasm fraction and a nitrocellulose membrane. In Panel C, the cytoplasmic and nuclear fractions of UV-C irradiated HeLa cells demonstrate that the DDB2 antibody does react with the DDB2 protein. This western blot was provided by Mr. Zheng Ke Li as a positive control for the anti-DDB2 antibody. The HeLa cells were allowed a three-hour recovery after radiation and the cell contents were separated into cytoplasmic and nuclear fractions.

Chapter 4. DISCUSSION AND CONCLUSIONS

In these studies, we have compared the differences in sensitivity to ultraviolet light (viability/metabolism) and the ability for DNA repair of the prematurely-aging HGPS fibroblasts and the normal BJ fibroblasts. Previously, the sensitivity of HGPS to ultraviolet light was relatively unknown. These cells accumulate DNA damage[5,8,9], which led us to hypothesize that they may show a greater sensitivity to UV irradiation than normal primary fibroblasts. We further hypothesized that the reason HGPS may show a higher sensitivity to ultraviolet light was potentially due to a difference in DNA repair and levels of repair-related proteins.

The first experiments utilized a Cell-Titer Blue Viability assay to determine the sensitivity of the cells to UV-B and UV-C irradiation after a three-day recovery. In order to assure that metabolic activity was an accurate indicator of the number of attached, viable cells, a Sybr Green assay also was performed as a measure of DNA contained per culture well. The results from each of these assays supported one another. These assays for both UV-B and UV-C irradiation revealed no significant difference between the dose-related toxicity between HGPS and BJ cells. An analysis of covariance (ANCOVA) statistical approach was used to compare the growth response of the two different cell types after UV exposure. The result of these analyses (Figs. 5-7) negated our initial hypothesis that HGPS cells would show an immediately apparent greater sensitivity to UV exposure, since HGPS and BJ cells seemed to be equally affected by either UV-B or UV-C irradiation after a relatively short 3-day recovery time.

In a follow-up experiment a longer recovery period was utilized, so that the long-term effect of ultraviolet exposure could be determined. This study also utilized a lung carcinoma cell line, A549, as a positive control. A549 cells have been shown to repair 100% of (6-4) PP and 97% of CPD damage within 72 hours[8]. These transformed cells are expected to efficiently repair UV-C-induced DNA damage and quickly restart cell cycle transit. The results indicate that though slightly slower than A549 cells, the BJ cells repaired the DNA damage fairly quickly and the fibroblasts restarted cycle transit (Fig. 8). The HGPS cells, both young and old, exhibited a longer recovery time, with little cell growth even after four days. These data indicate that HGPS cells have a greater sensitivity at a molecular level to ultraviolet light in long-term recovery, suggesting a deficient DNA repair process which is manifested with longer recovery times.

Studies in our lab by another undergraduate, Ms. Nahid Mehraban, showed that BJ had

29

repaired only 50% of CPD damage and HGPS only 30% after 72 hours of recovery[8]. However, the long-term viability study showed the replication of BJ and HGPS began between three and four days, despite the persistence of CPD damage. These repair data plus the viability studies suggest that replication started/resumed in the presence of significant CPD damage. This led to the idea that differences in the trans-lesion synthesis (TLS) of DNA could be the cause of the greater sensitivity of HGPS to UV irradiation. Pol-η is a low-error trans-lesion DNA polymerase[2]. Therefore, the delay in HGPS cell recovery may be due to either an inactive form of this TLS enzyme or one that is inefficiently utilized by the cell. In BJ, it seems that the amount of DNA damage is directly related to the amount of Pol-η found in the chromatin after 2.5 days of recovery. During this period, the cells are actively undergoing nucleotide excision repair (NER) and DNA replication, which requires Pol-η for persistent DNA damage sites during replication over the CPD damage. If the DNA damage overwhelms the repair response, the cell may enter senescence and then apoptosis. This process is consistent with the results of the western blot analysis from the cells processed after four days of recovery (Fig. 11). The HGPS cells showed a dramatic decline in chromatin-associated Pol-η as the UV-C exposure increased. In the absence of UV-C exposure the highest level of Pol-η was observed in the old HGPS cells (passage 21). HGPS cells are characterized by their accumulation of DNA damage and sensitivity to environmental conditions. The high amount of Pol-η present after four days in the unexposed sample indicates the effort of the cell to bypass this endogenous damage during replication. BJ cells showed no significant differences between the 0, 10 or 20 J/m^2 UV-C exposures in the level of Pol-η. This indicates that UV-damaged BJ cells are less likely to undergo senescence and enter the apoptosis cascade than are HGPS cells.

The DDB-2 results indicate that the usage of DDB (containing DDB1 and DDB2) may be limited to early detection and assistance in NER, since its presence was not found in any sample after four days of recovery, but was found in HeLa samples following a three-hour recovery. Further studies at early recovery time points are required to determine if there is a difference in DDB-2 amounts between the cell types. Another possibility is that DDB2 may be present in the cytoplasmic fractions of HGPS and/or BJ and could be investigated in future studies. A difference here could indicate a difference between HeLa cells and BJ and HGPS.

In conclusion, these studies revealed a difference in UV sensitivity between BJ and HGPS cells, with HGPS having a greater sensitivity to ultraviolet light. Although this was not evident

after a three-day recovery, it became more obvious with longer recovery periods where HGPS cells lagged further behind the BJ cells. When looking at the molecular level and Pol-η protein status, other differences between BJ and HGPS cells were observed; however, more studies need to be done and at different recovery periods with older HGPS to determine if there is a difference prior to cells entering senescence.

The specific aims of this research were to describe underlying mechanisms that either accelerate or slow the aging process in HGPS patients. One obvious deficiency is a slower DNA repair response and/or a deficiency in DNA replication over persistent bulky DNA adducts. This may reflect an ineffective form of Pol-η in the HGPS cells, either due to lower enzyme activity or an altered subcellular distribution. Further experiments can be done to investigate a potential difference in DDB-2 levels. Although HGPS is a complex and fatal syndrome, experiments aiming to better understand it and perhaps to find treatments for HGPS patients are vital. In addition to HGPS, slowing the overall aging process for all people gives extreme importance to these studies, as prolonging life by targeting and improving DNA repair lends promise to people nationwide.

Personal Acknowledgements

Academic and Financial Contributions

Bibliography

[1]Taylor C., Stern, R., Leyden, J., Gilchrest, B. 1990. "Photoaging/Photodamage and
   Photoprotection" J. of American Academy of Dermatology, 22:1-15.

[2]Skoneczna, A., McLyntyre, J., Skoneczny, M., Policinska, Z., Sledziewska-Gojska, E. 2007.
   Polymerase eta is a Short-lived, Proteasomally Degraded Protein that Is Temporarily
   Stabilized Following UV Irradiation in Saccharomyces cerevisiae. Journal of Molecular
   Biology, 366: 1074-1086.

[3]Stary, A., Sarasin, A. 2002. Molecular mechanisms of UV-induced mutations as revealed
   by the study of DNA polymerase η in human cells. Research in Microbiology, 153: 441-
   445.

[4]Laposa, R., Feeney, L., Crowley, E., de Feraudy, S., Cleaver, J. 2007. p53 suppression
   overwhelms DNA polymerase deficiency in determining the cellular UV DNA damage
   response. DNA Repair, (6) 12:1794-1804.

[5]Mounkes, L., Stewart, C. 2004. Aging and Nuclear Organization: lamins and progeria. Cell
   Biology, 16: 322-327.

[6]Inoki, T., Yamagami, S., Inoki, Y., Tsuru, T., Hamamoto, T., Kagawa, Y., Mori, T., Endo, H.
   2004. Human DDB2 splicing variants are dominant negative inhibitors of UV-damaged
   DNA repair. Biochemical and Biophysical Research Communications, 314: 1036-1043.

[7]Stubbert, L., Smith, J., Hamill, J., Arcand, T., McKay, B. 2009. The anti-apoptotic role for p53
   following exposure to ultraviolet light does not involve DDB2. Mutation Research, 663:
   69–76.

[8]Johnson, M., Mehraban, N. 2010. Comparing the effects of premature aging as related to DNA
   damage and repair. Midwest DNA Repair Symposium Poster Presentation. Louisville,

KY.

[9]Shell, M., Li, Z., Shkriabai, N., Kvaratskhelia, M., Brosey, C., Serrano, M., Chazin, W.,
   Musich, P., Zou, Y. 2009. Checkpoint kinase ATR promotes nucleotide excision repair of
   UV-induced DNA damage via physical interaction with xeroderma pigmentosum group
   A. J Biol Chem. 284 (36) 24213-22.

[10]Coldspring Harbor Laboratory Press. 2011. SDS loading buffer (5X).
   Cold Spring Harb Protoc; 2010; doi:10.1101/pdb.rec12340.

[11]Sancar, A., Lindsey-Boltz, L. A., Unsal-Kacmaz, K.; Linn, S. 2004. "Molecular mechanisms of
   mammalian DNA repair and the DNA damage checkpoints." Annu Rev Biochem **73**: 39-
   85.